

## Observation of a second $\pi h_{11/2} \otimes \nu h_{11/2}$ band in $^{126}\text{La}$

K. Y. Ma (马克岩),<sup>1,2</sup> J. B. Lu (陆景彬),<sup>1,\*</sup> S. P. Ruan (阮圣平),<sup>2</sup> D. Yang (杨东),<sup>1</sup> J. Li (李剑),<sup>1</sup> Y. Z. Liu (刘运祚),<sup>1</sup> Y. J. Ma (马英君),<sup>1</sup> X. G. Wu (吴晓光),<sup>3</sup> Y. Zheng (郑云),<sup>3</sup> and C. Y. He (贺创业)<sup>3</sup>

<sup>1</sup>College of Physics, Jilin University, Changchun 130023, China

<sup>2</sup>College of Electronic Science & Engineering, Jilin University, Changchun 130023, China

<sup>3</sup>China Institute of Atomic Energy, Beijing 102413, China

(Received 9 March 2013; revised manuscript received 7 October 2013; published 14 November 2013; corrected 4 December 2013)

High-spin states of  $^{126}\text{La}$  have been populated using the  $^{116}\text{Sn}(^{14}\text{N}, 4n)^{126}\text{La}$  reaction at a beam energy of 77 MeV. A side band linking to the known yrast  $\pi h_{11/2} \otimes \nu h_{11/2}$  band is observed.  $B(M1)/B(E2)$  ratios and alignments of the side band and DCO ratios of linking transitions between the side band and the yrast band suggest that the side band has the same  $\pi h_{11/2} \otimes \nu h_{11/2}$  configuration as that of the yrast band, and thus the side band is a second  $\pi h_{11/2} \otimes \nu h_{11/2}$  band in  $^{126}\text{La}$ . The separation energy,  $\Delta E(I) = E(I)_{\text{side}} - E(I)_{\text{yrast}}$ , between the side band and the yrast band at the same spin, and the energy staggering parameter  $S(I)$  of the second  $\pi h_{11/2} \otimes \nu h_{11/2}$  band in  $^{126}\text{La}$  are compared to those of other odd-odd La isotopes. The variation trends of  $\Delta E(I)$  and  $S(I)$  both suggest that it is reasonable to interpret the second  $\pi h_{11/2} \otimes \nu h_{11/2}$  band in  $^{126}\text{La}$  as an excited  $\pi h_{11/2} \otimes \nu h_{11/2}$  band as proposed for  $^{124}\text{La}$  rather than to interpret it as a partner band of a near degenerate chiral doublet band as done for  $^{128-134}\text{La}$ .

DOI: 10.1103/PhysRevC.88.057302

PACS number(s): 21.10.Re, 23.20.En, 23.20.Lv, 27.60.+j

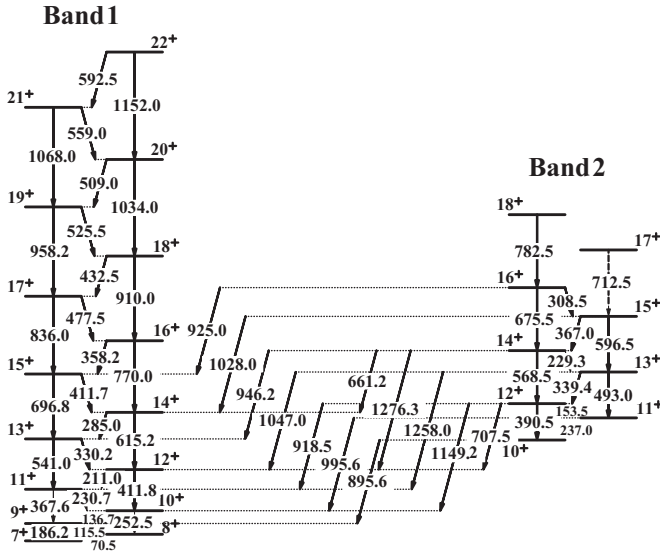
A second  $\pi h_{11/2} \otimes \nu h_{11/2}$  band has been reported in  $^{124}\text{La}$  [1],  $^{128}\text{La}$  [2],  $^{130}\text{La}$  [3],  $^{132}\text{La}$  [4], and  $^{134}\text{La}$  [5]. In the cases of  $^{128-134}\text{La}$  [2–5], the second  $\pi h_{11/2} \otimes \nu h_{11/2}$  band and the yrast  $\pi h_{11/2} \otimes \nu h_{11/2}$  band were cited as partners of near degenerate chiral doublet bands resulting from chiral symmetry breaking that occurred in triaxially deformed odd-odd nuclei [6]. In the case of  $^{124}\text{La}$  [1], the second  $\pi h_{11/2} \otimes \nu h_{11/2}$  band was considered to be an excited band of the yrast  $\pi h_{11/2} \otimes \nu h_{11/2}$  band, where two signature components of the second  $\pi h_{11/2} \otimes \nu h_{11/2}$  band were interpreted as resulting from the coupling of an unfavored signature component of the  $\pi h_{11/2}$  proton orbital with two signature components of the  $\nu h_{11/2}$  neutron orbital, while the two signature components of the yrast  $\pi h_{11/2} \otimes \nu h_{11/2}$  band were interpreted as resulting from the coupling of a favored signature component of the  $\pi h_{11/2}$  proton orbital with two signature components of the  $\nu h_{11/2}$  neutron orbital. Up to now, no experimental data on a second  $\pi h_{11/2} \otimes \nu h_{11/2}$  band in  $^{126}\text{La}$  is available. This report presents the results of our experimental study on a second  $\pi h_{11/2} \otimes \nu h_{11/2}$  band in  $^{126}\text{La}$ .

High-spin states of  $^{126}\text{La}$  were populated through the  $^{116}\text{Sn}(^{14}\text{N}, 4n)^{126}\text{La}$  reaction at a beam energy of 77 MeV. The  $^{116}\text{Sn}$  target, with an enrichment of 92.8% and a thickness of 3.2 mg/cm<sup>2</sup>, was rolled onto a 12.75 mg/cm<sup>2</sup> lead backing. The beam was provided by the HI-13 tandem accelerator at China Institute of Atomic Energy (CIAE) in Beijing. The  $\gamma$ - $\gamma$  coincidence data were recorded by the use of the detecting system consisting of nine Compton-suppressed high-purity germanium (HPGe) detectors, two HPGe planar detectors, and one clover-type detector. These Ge detectors in the array were placed at 90°, ±37°, ±30°, and ±60° relative to the beam direction. A total of  $4.5 \times 10^8$   $\gamma$ - $\gamma$  coincidence events

were recorded. The data were sorted into a symmetrized  $\gamma$ - $\gamma$  coincidence matrix and a directional correlation from oriented states (DCO) matrix, and the DCO matrix was created by sorting the detectors at ±30° and ±37° on one axis and the detectors at ~90° on the other. DCO ratios were obtained from spectra gated either on quadrupole or dipole transitions. For our detector array, when gating on a stretched quadrupole transition, the DCO ratio of the measured transition is around 1.0 for a stretched quadrupole transition or a nonstretched dipole transition and around 0.6 for a stretched dipole transition; and when gating on a stretched dipole transition, the DCO ratio of the measured transition becomes around 1.0 for a stretched dipole transition and around 1.7 for a stretched quadrupole transition.

High-spin states in  $^{126}\text{La}$  had previously been studied [7–9] and the yrast band was assigned to the  $\pi h_{11/2} \otimes \nu h_{11/2}$  configuration [8,9] and thus it has positive parity. The partial level scheme of  $^{126}\text{La}$  deduced from the present study is shown in Fig. 1. Properties and placements of related  $\gamma$  rays are listed in Table I. The level structure of the yrast band (band 1) is consistent with that of [9] except that the spin values of all levels in band 1 have been increased by  $2\hbar$  according to the systematics study [10] and the “extended” total Routhian surface (TRS) calculations [11]. Band 2 and linking transitions between bands 1 and 2 are observed in the present work. DCO ratios listed in Table I indicate that 918.5 and 946.2 keV linking transitions are of  $\Delta I = 1$  character and 1149.2 and 1276.3 keV linking transitions are of  $\Delta I = 2$  character. The observation of both  $\Delta I = 1$  and  $\Delta I = 2$  linking transitions between bands 1 and 2 implies that band 2 has a positive parity like that of band 1, and energies and spin values of the levels in band 2 are fixed relative to the levels in band 1 as shown in Fig. 1. It is found that when the internal conversion is not considered, 65.1%, 63.5%, and 60.8% of the total populating  $\gamma$  intensities of the 9<sup>+</sup> state in  $^{124}\text{La}$  [1],  $^{126}\text{La}$  (present work), and  $^{128}\text{La}$  [2] are missing, respectively. Possibly, due to the complexity of

\*ljb@jlu.edu.cn

FIG. 1. Partial level scheme of  $^{126}\text{La}$ .

the low-lying level structure in odd-odd nuclei, there are some depopulating low energy and/or highly converted  $\gamma$  rays were not observed. This is a problem which needs to be investigated further. A sample  $\gamma$ - $\gamma$  coincidence spectrum supporting the level scheme of Fig. 1 is shown in Fig. 2.

As mentioned above, the configuration of the yrast band (band 1) had previously been assigned as  $\pi h_{11/2} \otimes \nu h_{11/2}$  [8,9]. In order to discuss the configuration assignment of the side band (band 2), cranked shell model (CSM) calculations [12,13] were performed as shown in Fig. 3. The alignment of band 2 is shown in Fig. 4(a) along with that of band 1. The flat alignment of band 1 for  $\omega < 0.45$  MeV/ $\hbar$  clearly supports the  $\pi h_{11/2} \otimes \nu h_{11/2}$  configuration assignment for band 1 through blocking argument; i.e., neither the theoretical  $\omega_{\text{EF}}$  nor the  $\omega_{\text{ef}}$  alignment of Fig. 3 are evident. The similarity of alignments between band 2 and band 1, as shown in Fig. 4(a), tentatively suggests that band 2 has the same configuration as that of band 1. The experimental  $B(M1)/B(E2)$  ratios for bands 1

TABLE I. Energies, intensities, and DCO ratio of  $\gamma$  rays related to bands 1 and 2 and linking  $\gamma$  rays between them in  $^{126}\text{La}$ . The internal conversion is not taken into account in the present work.

$E_\gamma$ (keV)	$I_\gamma$	$R_{\text{DCO}}^a$	$R_{\text{DCO}}^b$	$I_i^\pi \rightarrow I_f^\pi$	Multipolarity
Band 1					
70.5				$8^+ \rightarrow 7^+$	(M1/E2)
115.5	32.1(28)	0.87(18)		$9^+ \rightarrow 8^+$	M1/E2
136.7	76.2(54)	0.92(22)		$10^+ \rightarrow 9^+$	M1/E2
186.2	2.1(6)	1.68(42)		$9^+ \rightarrow 7^+$	E2
211.0	78.0(66)	1.07(21)		$12^+ \rightarrow 11^+$	M1/E2
230.7 <sup>c</sup>	100.0(23)	1.03(21)		$11^+ \rightarrow 10^+$	M1/E2
252.5	17.0(34)	1.71(46)		$10^+ \rightarrow 8^+$	E2
285.0	30.5(32)	1.01(20)		$14^+ \rightarrow 13^+$	M1/E2
330.2	57.1(46)	0.92(18)		$13^+ \rightarrow 12^+$	M1/E2
358.2	8.5(26)	1.05(21)		$16^+ \rightarrow 15^+$	M1/E2
367.6	23.1(21)	1.74(41)		$11^+ \rightarrow 9^+$	E2
411.7	29.5(40)	0.96(19)		$15^+ \rightarrow 14^+$	M1/E2
411.8	53.1(51)	1.68(34)		$12^+ \rightarrow 10^+$	E2

TABLE I. (Continued.)

$E_\gamma$ (keV)	$I_\gamma$	$R_{\text{DCO}}^a$	$R_{\text{DCO}}^b$	$I_i^\pi \rightarrow I_f^\pi$	Multipolarity
432.5	2.1(11)	1.08(18)		$18^+ \rightarrow 17^+$	M1/E2
477.5	11.0(31)	0.95(22)		$17^+ \rightarrow 16^+$	M1/E2
509.0				$20^+ \rightarrow 19^+$	(M1/E2)
525.5	4.1(12)	0.89(28)		$19^+ \rightarrow 18^+$	M1/E2
541.0	34.2(72)	1.61(33)		$13^+ \rightarrow 11^+$	E2
559.0				$21^+ \rightarrow 20^+$	(M1/E2)
592.5				$22^+ \rightarrow 21^+$	(M1/E2)
615.2	67.1(82)	1.73(35)		$14^+ \rightarrow 12^+$	E2
696.8	51.2(61)	1.71(51)		$15^+ \rightarrow 13^+$	E2
770.0	38.1(45)	1.75(53)		$16^+ \rightarrow 14^+$	E2
836.0	28.1(36)	1.67(33)		$17^+ \rightarrow 15^+$	E2
910.0	24.3(32)	1.62(36)		$18^+ \rightarrow 16^+$	E2
958.2	15.1(42)	1.72(38)		$19^+ \rightarrow 17^+$	E2
1034.0	14.8(47)	1.77(41)		$20^+ \rightarrow 18^+$	E2
1068.0	5.8(21)	1.61(43)		$21^+ \rightarrow 19^+$	E2
1152.0	7.2(25)	1.58(36)		$22^+ \rightarrow 20^+$	E2
Band 2					
153.5	0.7(2)	0.96(38)		$12^+ \rightarrow 11^+$	M1/E2
229.3	3.1(11)	1.14(46)		$14^+ \rightarrow 13^+$	M1/E2
237.0				$11^+ \rightarrow 10^+$	(M1/E2)
308.5	1.5(5)			$16^+ \rightarrow 15^+$	(M1/E2)
339.4	4.8(13)	1.07(42)	0.55(13)	$13^+ \rightarrow 12^+$	M1/E2
367.0	3.5(11)			$15^+ \rightarrow 14^+$	(M1/E2)
390.5	2.1(8)			$12^+ \rightarrow 10^+$	(E2)
493.0	4.3(14)	1.79(52)		$13^+ \rightarrow 11^+$	E2
568.5	9.2(31)	1.76(60)	1.03(19)	$14^+ \rightarrow 12^+$	E2
596.5	5.7(19)	1.81(54)		$15^+ \rightarrow 13^+$	E2
675.5	4.1(14)			$16^+ \rightarrow 14^+$	(E2)
712.5				$17^+ \rightarrow 15^+$	(E2)
782.5	7.8(25)	1.74(58)		$18^+ \rightarrow 16^+$	E2
Linking transitions					
661.2	1.8(7)	0.89(38)		$14^+ \rightarrow 14^+$	M1/E2
707.5	1.4(4)	0.98(23)		$12^+ \rightarrow 12^+$	M1/E2
895.6				$10^+ \rightarrow 9^+$	(M1/E2)
918.5	4.8(16)	1.04(17)	0.56(9)	$12^+ \rightarrow 11^+$	M1/E2
925.0	1.6(5)			$16^+ \rightarrow 15^+$	(M1/E2)
995.6	2.3(8)	1.07(23)	0.63(11)	$11^+ \rightarrow 10^+$	M1/E2
946.2	4.3(15)	1.02(19)	0.57(8)	$14^+ \rightarrow 13^+$	M1/E2
1028.0				$15^+ \rightarrow 14^+$	(M1/E2)
1047.0	3.5(12)	1.12(25)		$13^+ \rightarrow 12^+$	M1/E2
1149.2	2.2(7)	1.71(45)	0.98(15)	$12^+ \rightarrow 10^+$	E2
1258.0	2.3(8)	1.76(42)		$13^+ \rightarrow 11^+$	E2
1276.3	3.1(11)	1.81(39)	1.06(16)	$14^+ \rightarrow 12^+$	E2

<sup>a</sup>DCO ratios listed here are obtained by setting the gate on mixed M1/E2 transitions.

<sup>b</sup>DCO ratios listed here are obtained by setting the gate on quadrupole transitions.

<sup>c</sup> $I_\gamma$  are normalized to the 230.7 keV  $\gamma$  ray in band 1 as 100.

and 2 are shown in Fig. 4(b) along with the theoretical estimates of the geometrical model [17] for the  $\pi h_{11/2} \otimes \nu h_{11/2}$  configuration. The general agreement between experimental results and theoretical estimates provides further support to the  $\pi h_{11/2} \otimes \nu h_{11/2}$  configuration assignment for both bands 1 and 2.

The separation energy between the states in the side band and the yrast band at the same spin,  $\Delta E(I) = E(I)_{\text{side}} - E(I)_{\text{yrast}}$ , in  $^{124-134}\text{La}$  are compared in Fig. 5. Within the

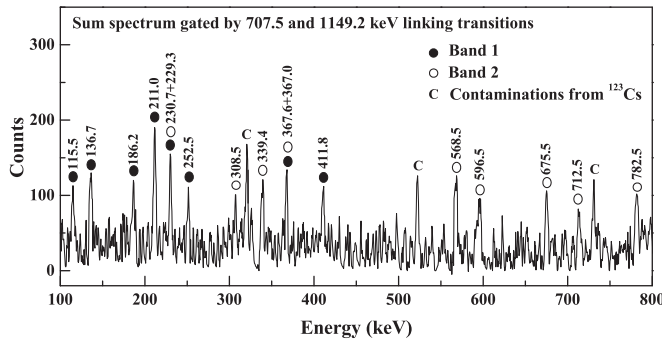


FIG. 2. Sample  $\gamma$ - $\gamma$  coincidence spectrum supporting the partial level scheme of  $^{126}\text{La}$  as shown in Fig. 1.

observed spin region, the magnitude and variation trend of  $\Delta E(I)$  of  $^{126}\text{La}$  is very similar to those of  $^{124}\text{La}$  [1], and quite different from those of  $^{128-134}\text{La}$  [2–5]. This fact suggests that it is reasonable to interpret the second  $\pi h_{11/2} \otimes \nu h_{11/2}$  band in  $^{126}\text{La}$  as the excited  $\pi h_{11/2} \otimes \nu h_{11/2}$  band, as proposed for  $^{124}\text{La}$  [1], rather than to interpret it as the partner band of chiral doublet bands, as for  $^{128-134}\text{La}$  [2–5].

An energy staggering parameter, defined as  $S(I) = E(I) - E(I-1) - 1/2[E(I+1) - E(I) + E(I-1) - E(I-2)]$ , is used to display the signature inversion phenomenon of a rotational band [1].  $S(I)$  of the yrast  $\pi h_{11/2} \otimes \nu h_{11/2}$  band in  $^{124}\text{La}$  [1],  $^{126}\text{La}$  (present work), and  $^{128}\text{La}$  [2] are shown

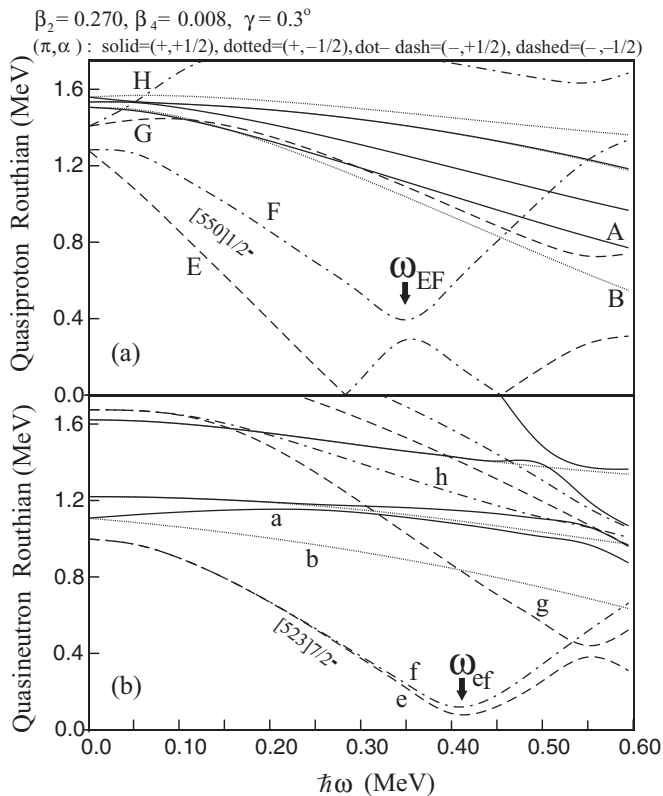


FIG. 3. Cranked shell model calculations for (a) quasiproton and (b) quasineutron Routhians. The deformation parameters shown at the top of the figure are determined by TRS calculations [14–16]. Interpretation of the lines is displayed at the top of the figure.

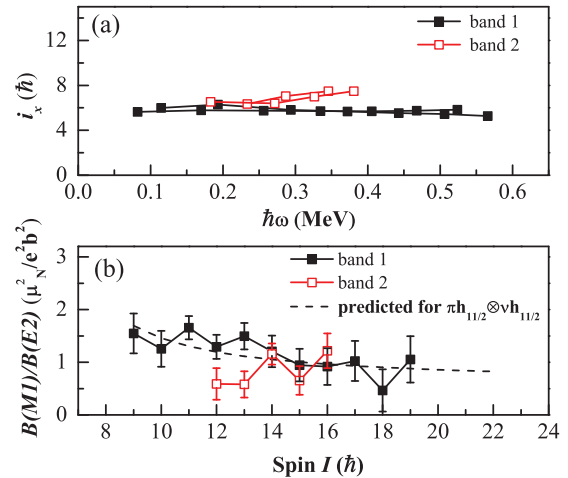


FIG. 4. (Color online) (a) Experimental alignment plots for bands 1 and 2 in  $^{126}\text{La}$ . The Harris parameters are  $J_0 = 22.7 \text{ MeV}^{-1} \hbar^2$ ,  $J_1 = 16.6 \text{ MeV}^{-3} \hbar^4$  [1]. (b) Comparison of experimental and predicted  $B(M1)/B(E2)$  values for bands 1 and 2. Parameters used in the calculations of the predicted values:  $Q_0 = 4.63 e b$ ,  $g_R = 0.452$ ,  $g_\pi(h_{11/2}) = 1.17$ ,  $g_\nu(h_{11/2}) = -0.21$ ,  $i_\pi(h_{11/2}) = 5.0$ ,  $i_\nu(h_{11/2}) = 3.0$ .

in Fig. 6(a).  $S(I)$  of the yrast  $\pi h_{11/2} \otimes \nu h_{11/2}$  band in  $^{124}\text{La}$  clearly indicates that below  $I_c = 18.5 \hbar$ , the expected favored signature component ( $\alpha = 1$  or odd spin) lies higher in energy than the expected unfavored signature component ( $\alpha = 0$  or even spin); and above  $I_c = 18.5 \hbar$ , the expected favored signature component ( $\alpha = 1$  or odd spin) lies lower in energy than the expected unfavored signature component ( $\alpha = 0$  or even spin), i.e., signature inversion occurs below  $I_c = 18.5 \hbar$  in the yrast  $\pi h_{11/2} \otimes \nu h_{11/2}$  band in  $^{124}\text{La}$  [1]. The  $I_c$  of the yrast band in  $^{126}\text{La}$  is about  $21.5 \hbar$ . For the second  $\pi h_{11/2} \otimes \nu h_{11/2}$  band in  $^{124}\text{La}$ , Fig. 6(b) clearly shows that below  $I_c = 18.5 \hbar$ , the expected favored signature component ( $\alpha = 0$  or even spin) lies lower in energy than the expected unfavored signature component ( $\alpha = 1$  or odd spin); and above  $I_c = 18.5 \hbar$ , the expected favored signature component ( $\alpha = 0$  or even spin) lies higher in energy than the expected

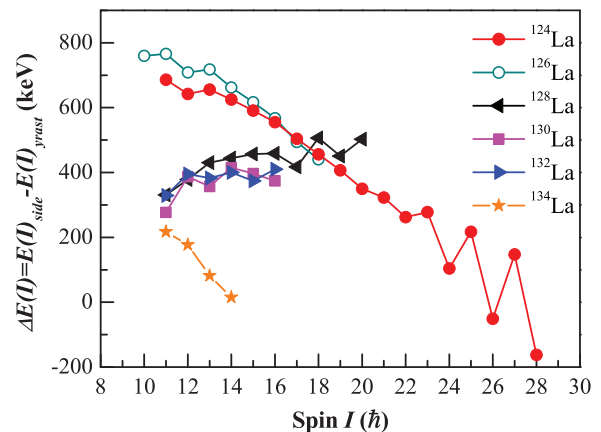


FIG. 5. (Color online)  $\Delta E(I) = E(I)_{\text{side}} - E(I)_{\text{yrast}}$  of the two bands in  $^{126}\text{La}$  compared with those in  $^{124}\text{La}$  [1],  $^{128}\text{La}$  [2],  $^{130}\text{La}$  [3],  $^{132}\text{La}$  [4], and  $^{134}\text{La}$  [5].

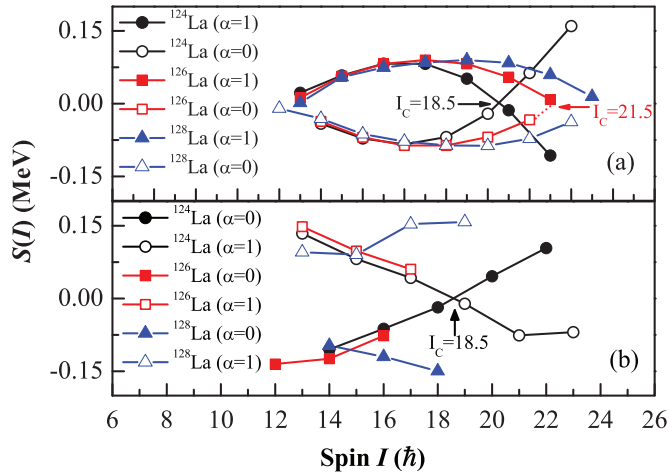


FIG. 6. (Color online) Energy staggering parameter  $S(I)$  vs spin  $I$  for the  $\pi h_{11/2} \otimes \nu h_{11/2}$  bands in  $^{124}\text{La}$  [1],  $^{126}\text{La}$  (present work), and  $^{128}\text{La}$  [2].

unfavored signature component ( $\alpha = 1$  or odd spin), i.e., signature inversion of the second  $\pi h_{11/2} \otimes \nu h_{11/2}$  band in  $^{124}\text{La}$  occurs above  $I_c = 18.5 \hbar$ , in contrast to that of the yrast  $\pi h_{11/2} \otimes \nu h_{11/2}$  band where signature inversion occurs below  $I_c = 18.5 \hbar$ .  $S(I)$  of the second  $\pi h_{11/2} \otimes \nu h_{11/2}$  band

in  $^{126}\text{La}$  and  $^{128}\text{La}$  [2] is also included in Fig. 6(b). Within the observed spin region, the variation trend of  $S(I)$  of the second  $\pi h_{11/2} \otimes \nu h_{11/2}$  band in  $^{126}\text{La}$  is very similar to that of the second  $\pi h_{11/2} \otimes \nu h_{11/2}$  band in  $^{124}\text{La}$  and quite different from that of  $^{128}\text{La}$ . This fact once again suggests that it is reasonable to interpret the second  $\pi h_{11/2} \otimes \nu h_{11/2}$  band in  $^{126}\text{La}$  as the excited  $\pi h_{11/2} \otimes \nu h_{11/2}$  band as proposed in  $^{124}\text{La}$  [1] rather than to interpret it as the partner band of a chiral doublet band as done for  $^{128-134}\text{La}$  [2–5]. Finally, this interpretation is also supported by the TRS calculations which predict that  $^{126}\text{La}$  has an axial quadrupole deformation, as indicated in Fig. 3, while a triaxial shape is needed for the chiral doublet bands to appear.

In summary, a second  $\pi h_{11/2} \otimes \nu h_{11/2}$  band has been identified in  $^{126}\text{La}$  through the reaction  $^{116}\text{Sn}(^{14}\text{N}, 4n)^{126}\text{La}$  at a beam energy of 77 MeV. It is observed that within the observed spin region, the variation trends of  $\Delta E(I)$  and  $S(I)$  both suggest that it is reasonable to interpret the second  $\pi h_{11/2} \otimes \nu h_{11/2}$  band in  $^{126}\text{La}$  as an excited  $\pi h_{11/2} \otimes \nu h_{11/2}$  band as proposed for  $^{124}\text{La}$  rather than to interpret it as a partner band of near degenerate chiral doublet bands as proposed for  $^{128-134}\text{La}$ .

This work is supported by the National Natural Science Foundation of China under Grant No. 11075064.

- [1] H. J. Chantler *et al.*, *Phys. Rev. C* **66**, 014311 (2002).  
 [2] K. Y. Ma, J. B. Lu, D. Yang, H. D. Wang, Y. Z. Liu, X. G. Wu, Y. Zheng, and C. Y. He, *Phys. Rev. C* **85**, 037301 (2012).  
 [3] T. Koike, K. Starosta, C. J. Chiara, D. B. Fossan, and D. R. LaFosse, *Phys. Rev. C* **63**, 061304 (2001).  
 [4] K. Starosta *et al.*, *Phys. Rev. Lett.* **86**, 971 (2001).  
 [5] R. A. Bark, A. M. Baxter, A. P. Byrne, G. D. Dracoulis, T. Kibédi, T. R. McGoram, and S. M. Mullins, *Nucl. Phys. A* **691**, 577 (2001).  
 [6] S. Frauendorf and J. Meng, *Nucl. Phys. A* **617**, 131 (1997).  
 [7] M. A. Quader, C. W. Beausang, P. Chowdhury, U. Garg, and D. B. Fossan, *Phys. Rev. C* **33**, 1109 (1986).  
 [8] B. M. Nyakó, J. Gizon, D. Barnéoud, A. Gizon, M. Józsa, W. Klamra, F. A. Beck, and J. C. Merdinger, *Z. Phys. A* **332**, 235 (1989).  
 [9] J. Timár *et al.*, *Eur. Phys. J. A* **7**, 7 (2000).  
 [10] Y. Z. Liu, J. B. Lu, Y. J. Ma, S. G. Zhou, and H. Zheng, *Phys. Rev. C* **54**, 719 (1996).  
 [11] F. R. Xu, W. Satula, and R. Wyss, *Nucl. Phys. A* **669**, 119 (2000).  
 [12] W. Nazarewicz, J. Dudek, R. Bengtsson, and I. Ragnarsson, *Nucl. Phys. A* **435**, 397 (1985).  
 [13] S. Cwiok, J. Dudek, W. Nazarewicz, W. Skalski, and T. Werner, *Comput. Phys. Commun.* **46**, 379 (1987).  
 [14] R. Wyss, J. Nyberg, A. Johnson, R. Bengtsson, and W. Nazarewicz, *Phys. Lett. B* **215**, 211 (1988).  
 [15] W. Nazarewicz, G. A. Leander, and J. Dudek, *Nucl. Phys. A* **467**, 437 (1987).  
 [16] W. Nazarewicz, R. Wyss, and A. Johnson, *Nucl. Phys. A* **503**, 285 (1989).  
 [17] F. Dönau, *Nucl. Phys. A* **471**, 469 (1987).